



New insights into the downregulation of cytochrome P450 2E1 via nuclear factor κ B-dependent pathways in immune-mediated liver injury

Huiqiong Zou ^{a,1}, Yingying Cao ^{a,1}, Peipei Hao ^{a,1}, Ziqi Jin ^a, Ruifeng Ding ^b,
Xuefeng Bai ^c, Kun Zhang ^{a,**}, Yongzhi Xue ^{a,*}

^a Institute of Pharmacokinetics and Liver Molecular Pharmacology, Department of Pharmacology, Baotou Medical College, No. 31 Jianshe Road, Donghe District, Baotou 014060, China

^b Department of Gastroenterology, First Affiliated Hospital, Baotou Medical College, No. 41 linyin Road, Kundurun District, Baotou 014010, China

^c Department of Pathology, Baotou Cancer Hospital, No. 18 Tuanjie Street, Qingshan District, Baotou 014000, China

ARTICLE INFO

Keywords:

Immune-mediated damage
Nuclear factor kappa B
Ammonium pyrrolidine dithiocarbamate
Cytochrome P450 2E1
Bacillus Calmette–Guerin
Post-translational modification

ABSTRACT

The extent of immune-mediated hepatic damage (such as in viral hepatitis) is characterised by the downregulation of cytochrome P450s (CYPs), a class of drug-metabolising enzymes. However, whether this downregulation aids liver cells in maintaining their homeostasis or whether the damage is aggravated remains largely unexplored. Herein, we evaluated the effects of phosphorylation mediated by the protein kinase C (PKC)/cAMP-response element binding protein (CREB) and nitration mediated by inducible nitric oxide synthase (iNOS) on the downregulation of CYP2E1 during immune-mediated liver injury. Additionally, we investigated the regulatory mechanism mediated by the nuclear factor κ B (NF- κ B). The rat model of immune-mediated liver injury was replicated by administering a single i.v. injection of Bacillus Calmette–Guerin (BCG, 125 mg/kg) vaccine and three i.p. injections of ammonium pyrrolidine dithiocarbamate (25, 50, 100 mg/kg/d, days 11, 12, and 13); blood was then collected on day 14. Subsequently, the livers were extracted to identify the different pharmacokinetic and biochemical indicators involved in the process. Our study reports new findings on the dependence between PKC-mediated CREB phosphorylation in the anti-inflammatory pathway and nitration emergency induced by iNOS in pro-inflammatory pathways in the NF- κ B pathway. The interaction of these two pathways leads to the downregulation and recovery of CYP2E1, thus alleviating inflammation and nitration stress. Our results confirm that BCG-mediated downregulation of CYP2E1 is linked to iNOS-induced nitration and PKC/NF- κ B-mediated CREB phosphorylation, and that NF- κ B is an important target in this process. These findings suggest that the downregulation of CYP2E1 may be an autonomous process characteristic of liver cells, helping them adapt to environmental changes, alleviate further hypoxia in inflamed tissues, and minimise exposure to toxic and harmful metabolites.

* Corresponding author.

** Corresponding author.

E-mail addresses: Kunzhang2623@163.com (K. Zhang), xyzhxyzh68@sohu.com (Y. Xue).

¹ These authors contributed equally to the work.

<https://doi.org/10.1016/j.heliyon.2023.e22641>

Received 6 June 2023; Received in revised form 6 October 2023; Accepted 15 November 2023

Available online 19 November 2023

2405-8440/© 2023 The Authors. Published by Elsevier Ltd. This is an open access article under the CC BY-NC-ND license (<http://creativecommons.org/licenses/by-nc-nd/4.0/>).

1. Introduction

The liver is the primary site of metabolic clearance, eliminating most drugs via hepatic cytochrome P450 (CYP)-dependent metabolism. Infection and inflammation induce the downregulation of CYPs [1,2]. Whether the downregulation of CYPs promotes liver cell homeostasis or aggravates the damage remains unclear, and the mechanisms underlying their downregulation remains unelucidated [3,4].

We have previously shown the involvement of transcriptional and post-transcriptional regulation of CYP2E1 in immune-mediated liver injury [5]. The mechanisms underlying its post-translational modification (PTM) and downregulation have been critical topics in liver immunopharmacology. Studies have investigated PTMs of drug-metabolising enzymes, including phosphorylation (CYP2D6, 2E1, 3A4, 11A1, 17A1, and 19A1) and nitration (CYP4A) [6], which can lead to loss or enhancement of protein function [7]. Phosphorylation is implicated in inflammation and immunity, and several CYP subtypes (CYP2C, CYP2E, CYP1A, CYP2B, and CYP3A) engage in phosphorylation. Protein kinases involved in CYP phosphorylation include protein kinase C (PKC), protein kinase A (PKA), and calmodulin-dependent protein kinase II (CaMKII) [8]. PKC-induced phosphorylation of CYP results in loss of function, and the activities of CYP2B1 and CYP2E1 decrease upon cAMP-dependent phosphorylation of enzymes [9]. The cAMP/PKC/cAMP-response element binding protein (CREB) pathway interacts with nuclear factor κ B (NF- κ B) to regulate inflammatory pathways and affect CYP2E1 expression and activity.

In immune-mediated liver injury, high nitrate levels produced by nitric oxide (NO) synthase activity induce CYP2E1 nitration, producing excessive nitrogen free radicals, which interact with the iron-sulphur cluster of CYP2E1 to form NO-Fe-nitrosoheme and denature proteins. The tyrosine site of CYP2E1 is vulnerable to peroxynitrite attack and subsequent 3-nitrotyrosine (3-NT) formation, a marker of peroxynitrite-mediated nitration-induced stress damage [10], which leads to the decreased metabolic activity of CYP2E1 and downregulated expression [2,11]. The downregulation of CYP2E1 is observed in almost all cases of immune-mediated liver injury, a leading factor for the development of viral hepatitis, cirrhosis, and hepatocellular carcinoma [12–14]. It undergoes PTM via phosphorylation or nitration, subsequently metabolising endogenous substances, chemical poisons, and drugs to modulate the degree of exposure, likely hastening the damage process and facilitating drug interactions [15].

Herein, we used the Bacillus Calmette–Guerin (BCG) vaccine to induce autoimmune liver injury in rats to evaluate the role of reduced CYP2E1 expression. BCG infection activates macrophages and T lymphocytes in the liver, releasing pro-inflammatory cytokines such as interleukin-1 β , tumour necrosis factor- α , and interferon- γ , and has been shown to be a cell-mediated immune response [5, 16]. Based on our prior investigations, we explored the mechanisms underlying NF- κ B-mediated regulation of PKC/CREB phosphorylation and inducible nitric oxide synthase (iNOS)-mediated nitration. We also studied the effects of these pathways on CYP2E1 downregulation in immune-mediated liver injury. We further examined the relationship between inflammation-associated pathways and the downregulation of oxidases to investigate whether CYP2E1 downregulation is an adaptive change maintaining liver cell homeostasis. We aimed to explore the mechanisms underlying CYP2E1 downregulation in immune-associated liver injury to gain insights into developing therapeutic strategies for liver diseases.

2. Materials and methods

2.1. Ethics statement

All animal experiments complied with the ARRIVE guidelines, and the Ethics Committee at Baotou Medical College approved all experimental protocols of this study (approval no.: 20210405). All methods were performed following the relevant guidelines and regulations. The animal model used in this study was the Sprague–Dawley rat. All animals were assessed as healthy before the commencement of the experiments. Animals were monitored before and following every injection ensuring there were no abnormalities in weight (>10 %), appearance (fur), or behaviour (vocalisation, respiration, and movements). All efforts were made to alleviate any animal suffering. They were handled by experienced researchers in such a way as to minimise stress before being terminally anaesthetised.

2.2. Experimental animals and reagents

We obtained 8- to 9-week-old male Sprague–Dawley rats weighing approximately 200 g from the Department of Laboratory Animal Science of Inner Mongolia University. The *Mycobacterium bovis* BCG vaccine (60 mg, batch number: 2019-1) was obtained from the National Institute for the Control of Pharmaceutical and Biological Products (Beijing, China). Ammonium pyrrolidine dithiocarbamate (PDTC) (batch number: 851002) was purchased from Sigma-Aldrich (St. Louis, MO, USA). Enzyme-linked immunosorbent assay (ELISA) kits for measuring the levels of rat tumour necrosis factor- α (TNF- α), interleukin (IL)-1 β , phosphodiesterase (PDE4), and cAMP, BCA protein kit, the sodium dodecyl sulphate-polyacrylamide gel electrophoresis (SDS-PAGE) preparation kit, as well as rabbit polyclonal antibodies against CYP2E1 (catalogue number: PB0186), PKC (catalogue number: PBM0401), CREB (catalogue number: PB0513), phospho-CREB (P-CREB, catalogue number: P00577), NF- κ B (catalogue number: BA0610), glyceraldehyde-3-phosphate dehydrogenase (GAPDH; catalogue number: BA2913), and β -tubulin (catalogue number: A01857-1), were purchased from Wuhan Boster Biological Engineering Co. Ltd. (Hubei, China). The total RNA extraction kit, cDNA synthesis kit, and the 2X real-time qPCR Master Mix were purchased from Nanjing Bordi Biotechnology Co. Ltd (Nanjing, China). Other chemicals used in the present study were of analytical grades and were purchased from commercial sources.

2.3. Development of an animal model of immune-mediated liver injury

Animals were housed in groups of 4–6/cage with padding at 18–22 °C, 40–60 % humidity, 12-h light/dark cycle, and 10–15 air changes/h. Moreover, they were allowed ad libitum access to food and water. All rats were acclimatised for at least one week in the animal facility before the initiation of the experiments. The animals were divided randomly into the following five groups of 10 animals each, with a control (saline-treated) groups and four treatment groups, treated with a fixed dose of the BCG vaccine (125 mg/kg), with or without varying dosages of PDTC (25, 50, and 100 mg/kg/day). The five groups were as follows: (1) control (1 ml normal saline), (2) BCG, (3) BCG + low-dose PDTC (25 mg/kg), (4) BCG + intermediate-dose PDTC (50 mg/kg), and (5) BCG + high-dose PDTC (100 mg/kg). Normal saline and the BCG vaccine were administered via i.v. injections, whereas PDTC was administered via i.p. injections. The rats in the BCG-treated group were vaccine-administered only once on day 1. PDTC was injected on days 11, 12, and 13, and the rats were sacrificed on day 14. The animals were fasted for 12 h for orbital venous plexus blood collection and then euthanised by cervical dislocation on day 14. The livers were extracted for biochemical and histopathological examinations. A few of these livers were fixed in formaldehyde–alcohol solution (formaldehyde: alcohol = 1:9). Subsequently, paraffin-embedded sections of these fixed liver tissues were prepared for immunohistochemical or haematoxylin and eosin (H&E) staining. Other liver samples were snap-frozen in liquid nitrogen for further use in western blotting, high-performance liquid chromatography (HPLC), qPCR, and ELISA analyses.

2.4. Liver histopathology

Six samples from each group were fixed with 4 % paraformaldehyde and embedded in paraffin. Sections (each of 5.0 µm thickness) were prepared for H&E staining. Hepatic histopathological changes in H&E sections were observed under an optical Olympus CX23 microscope (Olympus, Tokyo, Japan).

2.5. Liquid chromatography–tandem mass spectrometry proteomic analyses

Proteomic analysis was performed at Shanghai Applied Protein Technology Co. Ltd (Zhongke, Shanghai, China) using liquid chromatography–tandem mass spectrometry [17]. Additional information on protein extraction and digestion, isolation, chromatographic conditions and mass spectrometry parameters, protein identification, quantification, and bioinformatics analysis is available in complementary materials.

2.6. Immunohistochemical evaluation of iNOS expression in rat liver

Immunohistochemical analysis was conducted to determine iNOS expression in rat liver following the instructions provided in the kit (Wuhan Boster Biological Engineering Co. Ltd. Hubei, China). The results were analysed using ImageScope software 12.3 (Aperio Technologies, San Diego, CA, USA).

2.7. Preparation of liver microsomes

The rats were fasted for 12 h with continuous access to water and then sacrificed by cervical dislocation. The livers were perfused, extracted, and snap-frozen. The tissue samples were thawed on ice and weighed. Samples were homogenised on ice in 0.05 M phosphate (pH 7.4) buffer (10 ml/g). The homogenate was centrifuged at $12,500 \times G$ for 20 min at 4 °C in a cryogenic ultracentrifuge. The supernatant was removed and centrifuged at $105,000 \times G$ and 4 °C for 60 min to obtain the fraction with the microsomal precipitate. This precipitate was used as the source of microsomes secreted by the liver. The final microsome pellet was suspended in 200 µl of PBS buffer. The microsomal suspension was frozen and stored at –80 °C for further analysis.

2.8. Measurement of CYP2E1 metabolic activity levels

The levels of CYP2E1 were measured following the protocol described in previous studies [5,18–20]. Briefly, to evaluate the metabolic activity of liver CYP2E1, *in vitro* microsomal incubation of the probe drug chlorzoxazone was used to detect the time-dependent changes in the probe drug. The total reaction volume was 200 µl, 100 µl each of liver microsomes and probe drugs, with Tris-HCl buffer added in succession. The reaction mix was incubated at 37 °C for 5 min, after which NADPH was added to initiate the reaction, and the reaction mix was incubated for another 45 min at 37 °C. Three volumes of ethyl acetate were added at 0 °C to stop the reaction. The mixture was vortexed for 5 min and then centrifuged at $10,000 \times G$ for 10 min at 4 °C. Approximately 2.5 ml of the supernatant was removed and dried under a stream of nitrogen at 40 °C. The residue was dissolved in 300 µl of mobile phase solution and injected into the HPLC system for analysis. The rate of generation of 6-OH-chlorzoxazone from chlorzoxazone was used to evaluate the metabolic activity of CYP2E1.

2.9. Western blotting

The liver tissues were weighed, and proteins were extracted following the instructions provided in the protein extraction kit (Wuhan Boster Biological Engineering Co. Ltd., Hubei, China). Equal amounts of proteins (30 µg) from each sample were loaded, resolved by SDS-PAGE, and blotted onto nitrocellulose paper (Wuhan Boster Biological Engineering Co. Ltd., Hubei, China). The levels

of CYP2E1 protein were detected by incubating the membrane with the anti-CYP2E1 antibody at a dilution of 1:200 at 4 °C overnight. CREB, P-CREB, PKC, NF- κ B, and inhibitor of NF- κ B subunit alpha ($\text{I}\kappa\text{B}\alpha$) were detected with anti-CREB, anti-P-CREB, anti-PKC, anti-NF- κ B, and anti- $\text{I}\kappa\text{B}\alpha$ antibodies, respectively, at a dilution of 1:200. Anti- β -tubulin (1:200) and anti-GAPDH were included as housekeeping controls. For chemiluminescence detection, the blots were incubated with goat anti-rat IgG at a dilution of 1:2000 conjugated to horseradish peroxidase and developed with hypersensitive ECL chemiluminescent substrate. The blot images were acquired using an Omega Lum C Gel imaging system, and band intensities were quantified using Fluor Chem 5500 software (Gel Company, San Francisco, CA, USA). The expression level of the control group was set to 1 for the analysis.

2.10. RNA extraction, cDNA synthesis, and quantitative reverse transcription polymerase chain reaction

Total RNA was prepared using an RNA fast200 extraction kit (Nanjing Bordi Biotechnology Co. Ltd, Nanjing, China) following the manufacturer's instructions. RNA concentration was determined by measuring absorbance at 260 nm. RNA purity and integrity were confirmed via denaturing formaldehyde-agarose gel electrophoresis. cDNA synthesis from total RNA was performed using the first-strand cDNA synthesis kit. Quantitative reverse transcription-polymerase chain reaction (qRT-PCR) was used to measure the relative expression of CYP2E1 and CREB mRNA using the ABI 7900 HT real-time PCR system (ABI, USA) and SyBr® Green Master Mix reagent (Biosystems Research Corp., Nanjing, China). The sequences used for qPCR amplification of the cDNAs are provided below. The forward and reverse primers used for the amplification of CYP2E1 were 5'-TGGATGCTGTGGTGCATGAGATCC-3' and 5'-

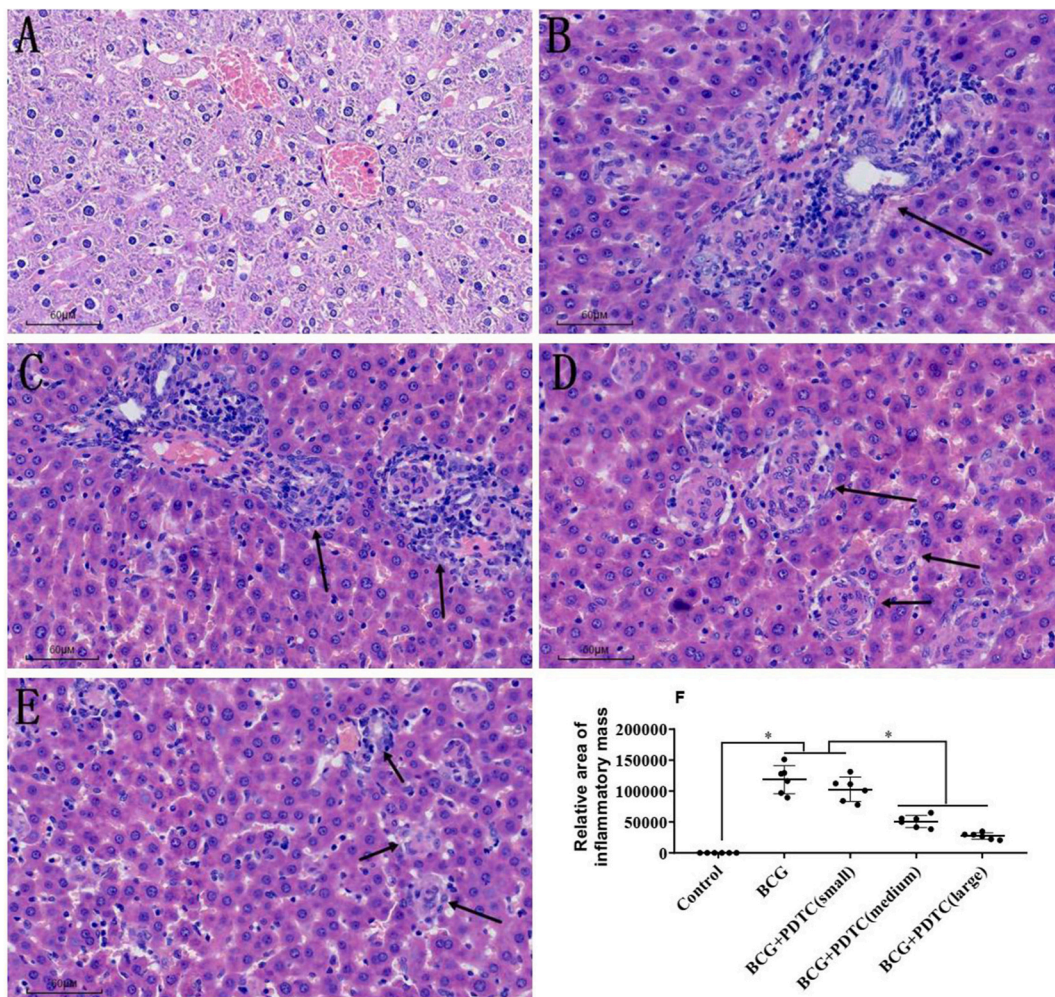


Fig. 1. Effects of ammonium pyrrolidine dithiocarbamate (PDTC) treatment on the distribution of inflammatory liver nodules in rats with immune-associated liver injury. (A) The control group shows normal hepatocyte structure. (B) Animals treated with the Bacillus Calmette-Guerin (BCG) vaccine alone demonstrate focal hyperplasia of macrophages, forming nodules. The nodules are scattered in several cases, with distinct boundaries from the surrounding liver cells. A small degree of lymphocyte infiltration may be seen during the specified period. The liver cells around the nodules show mild cellular oedema. (C-F) In addition, PDTC intervention inhibits liver inflammatory changes in a dose-dependent manner. Data related to nodule area are shown as mean \pm S.D., $n = 6$. The asterisks above the bars indicate differences between groups.

TCCTTGGAAACAGTATCTCT-3', respectively. The corresponding primers used for the amplification of CREB were 5'-GAAAG-CAGTGACGGAGGAGC-3' and 5'-TAACGCCATGGACCTGGACT-3', respectively. The forward primer for the amplification of GAPDH was 5'-AAGAAGGTGGTGAAGCAGGCATC-3', and the reverse primer was 5'-CAGCATCAAAGGTGAAGAGTG-3'. Values were normalised to the levels of GAPDH mRNA using the $\Delta\Delta C_t$ method, with its expression level in control samples arbitrarily set to 1.

2.11. Detection of IL-1 β , TNF- α , and 3-nitrotyrosine levels in rat liver using ELISA

The levels of IL-1 β , TNF- α , and 3-nitrotyrosine (3-NT) in rat livers were determined following the manufacturer's instructions using ELISA kits. A 0.2 g liver tissue sample was weighed and homogenised in PBS (1 ml, pH = 7.4), followed by centrifugation for 20 s (3500 \times G), and the supernatant was collected. A microplate reader was used to measure the absorbance of the samples in each well at 450 nm within 30 min following the instructions provided with the kit. Wells containing only the chromogenic substrate 3,30,5,50-tetramethylbenzidine (TMB) were used as blank controls. The absorbance of the standard and experimental samples was subtracted from the absorbance of the TMB control sample. The results were drawn based on the standard curve, followed by the determination of the linear regression equation used to calculate the respective concentrations of IL-1 β , TNF- α , and 3-NT in the liver homogenate.

2.12. Statistical analyses

The experimental results were expressed as mean \pm S.D. The data were subjected to analysis of variance (ANOVA) followed by Tukey's test using the SPSS 19.0 statistical software (IBM Corp., Armonk, NY, USA). Data homoscedasticity was evaluated using the Brown-Forsythe test. $P < 0.05$ was considered statistically significant.

3. Results

3.1. PDTC alleviates histopathological changes in immune-induced injury in rat livers

Activation of the NF- κ B pathway is essential for the induction of immune-mediated liver injury caused by the BCG vaccine. PDTC

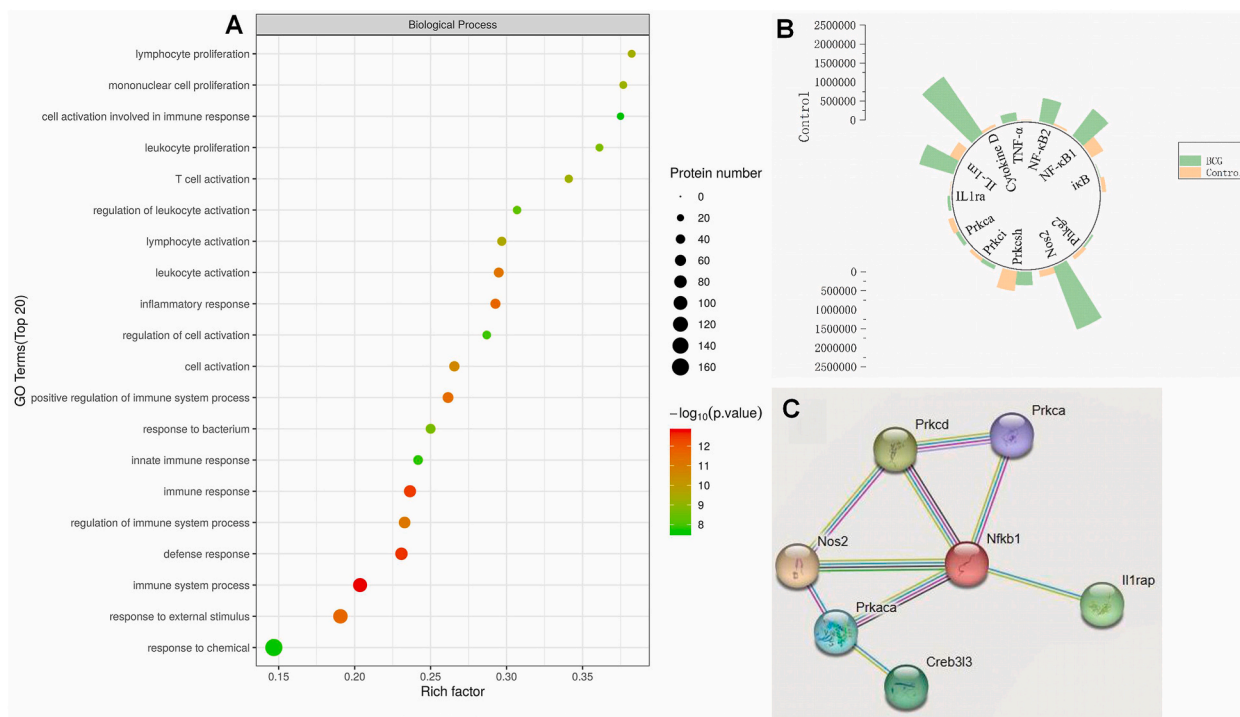


Fig. 2. Effects of BCG treatment on rat liver proteome. (A) Functionally enriched GO bubble map of biological processes in the control and BCG-treated groups shows that the closer the bubble is towards red, the more significant it is, the bigger the bubble, and the more protein there is. (B) Histogram of protein quantitative difference results. (C) Protein interaction map. Abbreviations: BCG, Bacillus Calmette-Guérin; GO, gene ontology; CYP, cytochrome P450; IkBKB, an inhibitor of nuclear factor kappa B kinase subunit beta; PHKG2, phosphorylase kinase γ subunit; NF- κ B1, nuclear factor kappa B subunit 1; NF- κ B2, nuclear factor kappa B subunit 2; TNF- α , tumour necrosis factor alpha; IL-1RN, interleukin-1 receptor antagonist; IL-1ra, interleukin-1 receptor access; NOS2, nitric oxide synthase 2; CREB3L3, cAMP-responsive element-binding protein 3-like 3. (For interpretation of the references to colour in this figure legend, the reader is referred to the Web version of this article.)

inhibited the effect of NF- κ B by hindering I κ B phosphorylation, thereby blocking the translocation of NF- κ B to the nucleus. Therefore, PDTC was employed to investigate liver pathology to determine the effect of NF- κ B activation on liver inflammation. The histology of rat livers in the control group showed normal morphology (Fig. 1A); however, after two weeks of BCG-mediated immune stimulation, H&E staining of liver tissues showed focal macrophage proliferation and nodule formation. We observed that the multiple nodules formed were scattered, with clear boundaries established from the surrounding liver cells, accompanied by a limited extent of lymphocyte infiltration in the nodule. The liver cells around the nodules showed mild cellular oedema (Fig. 1B). We also found that the inflammatory changes in the liver were inhibited in a dose-dependent manner upon PDTC administration (Fig. 1C–F).

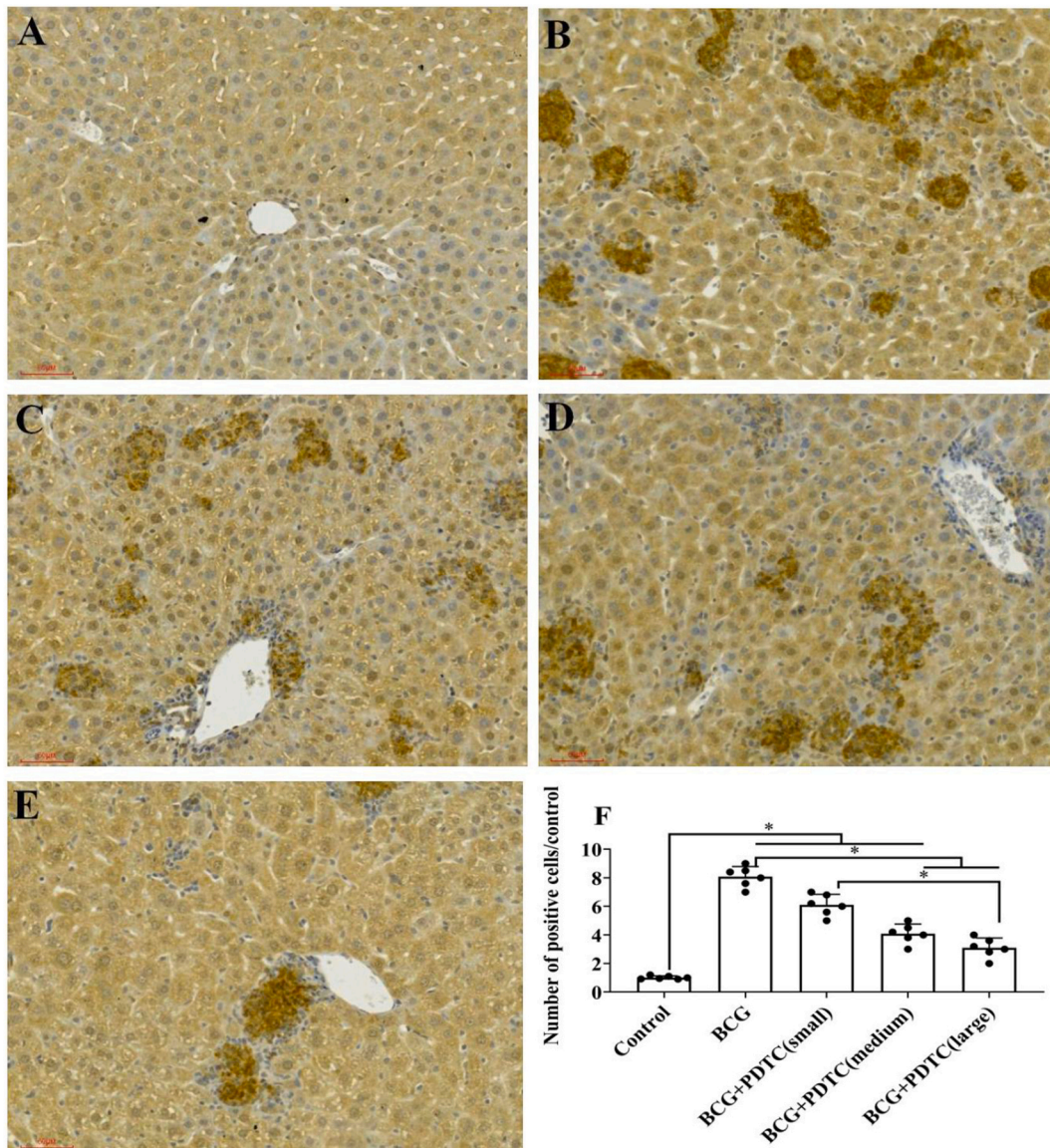


Fig. 3. Effects of ammonium pyrrolidine dithiocarbamate (PDTC) treatment on inducible nitric oxide synthase (iNOS) expression in rat livers with immune-mediated injury. Rats were administered injections of BCG (125 mg/kg, i.v. on day 1) or BCG (125 mg/kg, i.v. on day 1) + PDTC (25, 50, or 100 mg/kg/d, i.p. on days 11, 12, and 13). (A) Immunohistochemical staining of liver sections from each group of rats shows normal, clear liver morphology in the control group. (B) After two weeks of continuous BCG-mediated immunostimulation, the immunohistochemical staining of liver tissue shows that iNOS is expressed in the cytoplasm, as indicated by brown granules or flakes, and weakly expressed in the cytoplasm of hepatocytes. It is expressed strongly in the cytoplasm of macrophages. (C–F) PDTC treatment inhibits the induction of iNOS in the liver in a dose-dependent manner. The data relating to the brown-yellow positive staining area are shown as mean \pm S.D. compared with that in the control group, $n = 6$. The asterisks above the bars indicate differences between groups. (For interpretation of the references to colour in this figure legend, the reader is referred to the Web version of this article.)

3.2. Effects of BCG treatment on rat liver proteome

A total of 5521 proteins were detected, and 5353 proteins were quantified in the livers of rats in the control and BCG-vaccinated groups through proteomics. Functionally enriched Gene Ontology bubble maps showed an enhanced immune response in the BCG-treated group (Fig. 2A). Among the differentially expressed proteins, regulatory pathway proteins are discussed in this study. In addition, quantitative protein analysis showed that PKC and phospho-PKC were downregulated, with the NF- κ B, IL-1 β , and TNF- α pathways activated in the BCG-treated group compared with that in the control group (Fig. 2B). The interaction between proteins as determined in the bioinformatics analysis is shown in Fig. 2C.

3.3. PDTC inhibits the induction of iNOS in a dose-dependent manner in BCG-induced immune-mediated liver injury

Next, we evaluated the effects of nitration-induced liver stress on NF- κ B activation in immune-mediated liver injury. Hence, we investigated the effects of PDTC treatment on the expression of iNOS in rat liver. After two weeks of BCG-mediated immunostimulation, immunohistochemical staining of liver tissues showed a cytoplasmic expression of iNOS, as indicated by brownish-yellow granules or flakes. A weak positive stain for such structures was evident in the cytoplasm of hepatocytes; however, a robust expression was seen in the cytoplasm of the macrophages, with no expression detected in livers in the control group (Fig. 3A and B). Finally, we observed that PDTC treatment inhibited the induction of iNOS in the liver in a dose-dependent manner (Fig. 3C–F).

3.4. PDTC alleviates CYP2E1 downregulation in microsomes from rats with immune-mediated liver injury

Next, we investigated the metabolic activity of CYP2E1 at the microsomal level to elucidate the role of NF- κ B in its downregulation in immune-mediated liver injury by administering PDTC. The CYP2E1 protein regulates the generation of the 6-hydroxyl derivative of chlorzoxazone. Therefore, the conversion of chlorzoxazone to 6-OH-chlorzoxazone reflects the metabolic activity of CYP2E1. We performed a comparative analysis of the peak area obtained from HPLC analysis of the metabolites of the probe drug chlorzoxazone, the prototype drug, and total protein concentrations in the livers extracted from each group of rats. The *in vitro* metabolic rate in the rats in the BCG group was significantly lower than that in the rats in the control group ($P < 0.01$). Moreover, the metabolic rate gradually recovered as the dose of PDTC increased, particularly in the high-dose PDTC group; however, the rats in the control group retained their metabolic rates at the same level ($P < 0.01$) (Fig. 4).

3.5. NF- κ B/PKC/CREB pathway is involved in the downregulation of CYP2E1 in the livers of rats with immune-mediated liver injury

Next, we evaluated the expression of NF- κ B/I κ B α , PKC, CREB, P-CREB, and CYP2E1 to delineate phosphorylation-mediated CYP2E1 downregulation in immune-mediated liver injury. PDTC was simultaneously administered to the rats to determine the role of NF- κ B in this process. The western blots showed equal loading for the internal controls GAPDH or β -tubulin, which, in turn, indicated accurate protein estimation and confirmed similar expression levels of proteins in all samples. For the western blotting analysis, we set the expression levels of the control group to 1 and calculated the relative protein expression of the treatment groups (Fig. 5A–F). Our results showed that BCG-mediated immune stimulation significantly augmented CREB and NF- κ B expression (148 and 287 %, respectively, Fig. 5C and E); conversely, PDTC treatment reduced the expression of CREB and NF- κ B in a dose-dependent manner (Fig. 5A and E). In addition, BCG-mediated immune stimulation significantly inhibited the expression of PKC, P-CREB, CYP2E1, and I κ B α (55, 71, 57, and 47 %, respectively, Fig. 5A, B, D, and F); conversely, PDTC treatment restored the expression of PKC, P-CREB,

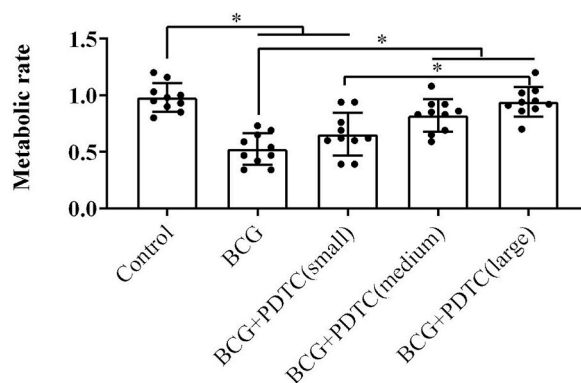


Fig. 4. Effects of ammonium pyrrolidine dithiocarbamate (PDTC) treatment on cytochrome P450 2E1 (CYP2E1) activity in liver microsomes from rats with immune-mediated liver injury. Rats were administered injections of BCG (125 mg/kg, i.v. on day 1) or BCG (125 mg/kg, i.v. on day 1) + PDTC (25, 50, or 100 mg/kg/d, i.p. on days 11, 12, and 13), and liver microsomes were collected. After *in vitro* incubation with microsomes, the metabolic rate was expressed as the ratio of 6-OH-chlorzoxazone to chlorzoxazone and weighted by the control group. Data represent the mean \pm S. D. of $n = 10$ rats. The asterisks above the bars indicate differences between groups.

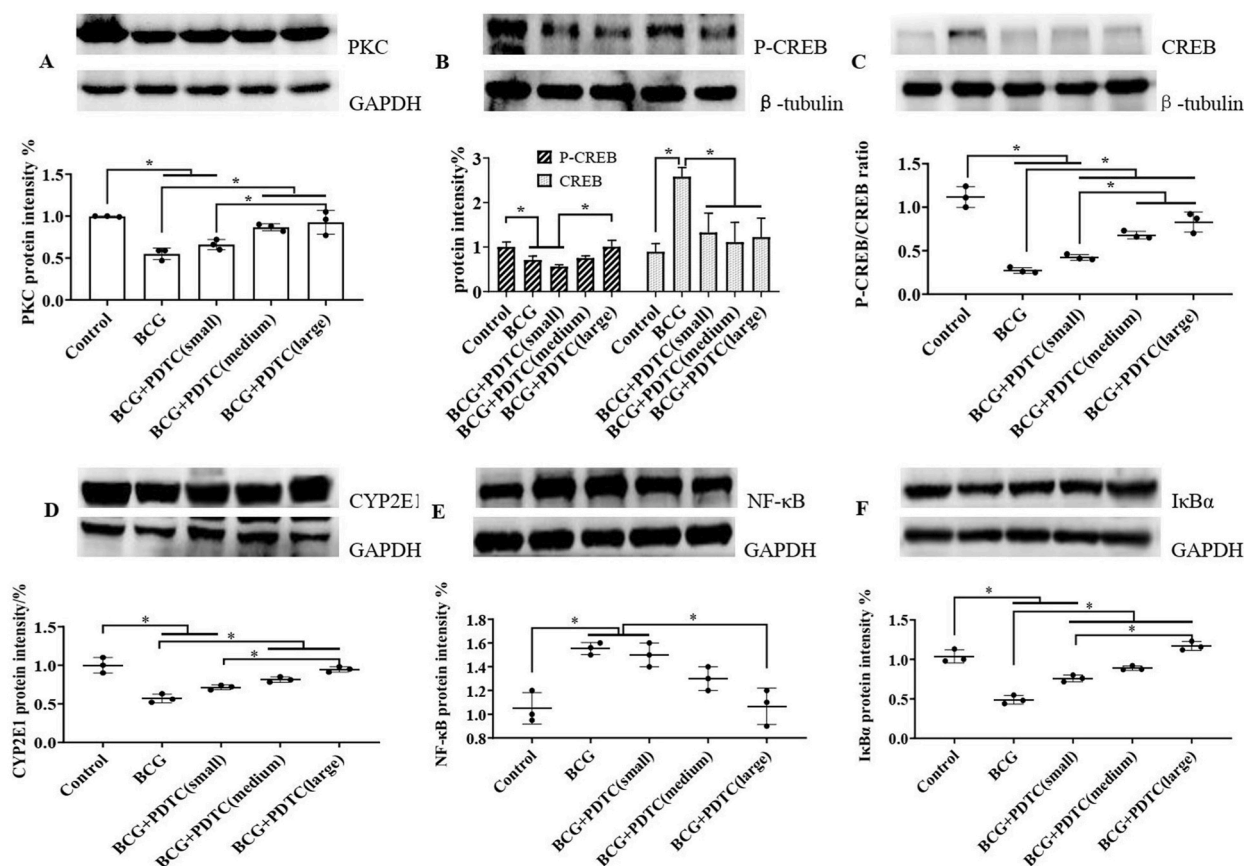


Fig. 5. Effects of PDTC treatment on the expression of PKC, CREB, P-CREB, CYP2E1, NF- κ B, and I κ B α in immune-mediated liver injury. Rats were administered injections of BCG (125 mg/kg, i.v. on day 1) or BCG (125 mg/kg, i.v. on day 1) + PDTC (25, 50, or 100 mg/kg/d, i.p. on days 11, 12, and 13). Liver proteins were extracted to determine the expression of PKC, CREB, P-CREB, CYP2E1, NF- κ B, and I κ B α . Equal amounts (30 μ g) of protein were subjected to SDS-PAGE followed by Western blot analysis using anti-PKC, anti-CREB, anti-P-CREB, anti-CYP2E1 anti-NF- κ B and anti-I κ B α antibodies. The results were normalised to the levels of GAPDH and β -tubulin. Western blotting images showing the protein expression of (A) PKC, (B) P-CREB, (C) CREB, (D) CYP2E1, (E) NF- κ B, and (F) I κ B α in the rat liver. Image Quant software was used to quantify expression. Data are expressed as the mean \pm S.D. of three independent experiments ($n = 3$). The asterisks above the bars indicate differences between groups. Comparisons between groups were performed using one-way ANOVA followed by Tukey's test. Abbreviations: PDTC, ammonium pyrrolidine dithiocarbamate; PKC, protein kinase C; CREB, cAMP-response element binding protein, P-CREB, phospho-CREB; CYP2E1, cytochrome P450 2E1; NF- κ B, nuclear factor κ B; I κ B α , an inhibitor of NF- κ B subunit alpha; BCG, Bacillus Calmette-Guérin; SDS-PAGE, sodium dodecyl sulphate-polyacrylamide gel electrophoresis; GAPDH, glyceraldehyde-3-phosphate dehydrogenase; ANOVA, analysis of variance.

CYP2E1, and I κ B α in a dose-dependent manner (Fig. 5A, B, D, and F).

3.6. Effects of PDTC treatment on the expression of CYP2E1 and CREB mRNA in the livers of rats with immune-mediated liver injury

Next, we used qRT-PCR to determine the effects of inhibition of NF- κ B activation on the expression of CYP2E1 and CREB in rat liver. After BCG-mediated immuno-stimulation, the expression of CYP2E1 decreased ($P < 0.01$); conversely, PDTC treatment gradually recovered the CYP2E1 expression profile, with the high-dose group recovering to a level similar to that of the control group ($P < 0.05$) (Fig. 6A). CREB mRNA expression increased significantly in rat livers in the BCG-treated group compared to that in the livers in the control group ($P < 0.01$). In addition, low, medium, and high doses of PDTC downregulated CREB expression, with the high-dose group showing the most significant difference ($P < 0.05$) (Fig. 6B). Correlation analysis of CREB mRNA and CYP2E1 mRNA showed a high degree of negative correlation ($P < 0.05$).

3.7. Inhibition of NF- κ B activation suppresses the upregulation of IL-1 β , TNF- α , 3-NT, PDE4, and cAMP in immune-mediated liver injury

Next, to elucidate the alterations in the expression profile of pro-inflammatory factors in immune-mediated liver injury and the effects of inhibiting NF- κ B activation, we used ELISA to determine the changes in the levels of IL-1 β and TNF- α in rat liver tissues. The results revealed an increase in the expression levels of IL-1 β and TNF- α in the liver tissues ($P < 0.05$) after 14 days of BCG injection.

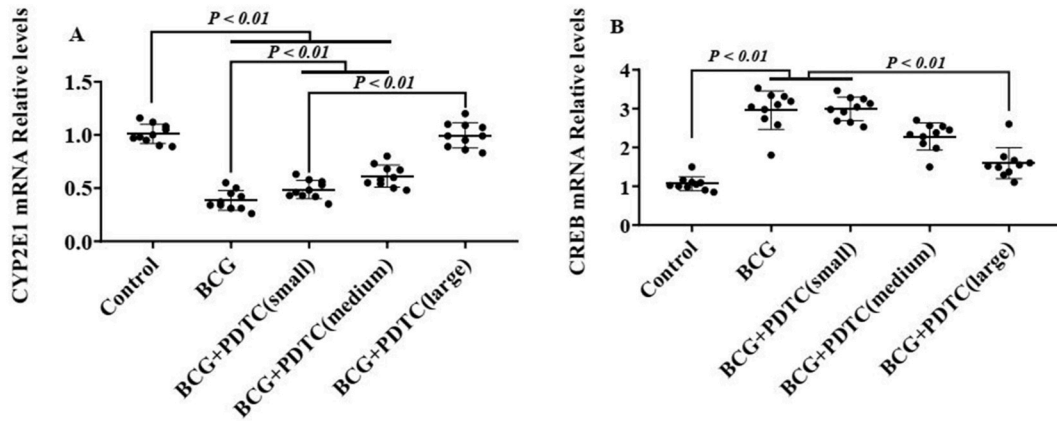


Fig. 6. Effects of ammonium pyrrolidine dithiocarbamate (PDTC) treatment on CYP2E1 and CREB mRNA expression in rats with immune-mediated liver injury. Rats were administered injections of BCG (125 mg/kg, i.v. on day 1) or BCG (125 mg/kg, i.v. on day 1) + PDTC (25, 50, or 100 mg/kg/d, i.p. on days 11, 12, and 13). (A) BCG-mediated immuno-stimulation decreases the expression of CYP2E1 ($P < 0.01$); conversely, PDTC treatment gradually recovers the CYP2E1 expression profile, with the high-dose group recovering to a level similar to that of the control group ($P < 0.05$). (B) Low, medium, and high doses of PDTC downregulate CREB expression, with the high-dose group showing the most significant difference ($P < 0.05$). Data represent the mean \pm S.D. of $n = 10$ rats. P -values above scatter charts indicate differences between groups. Comparisons between groups were performed using one-way ANOVA followed by Tukey's test.

Moreover, PDTC treatment decreased the levels of TNF- α and IL-1 β in a dose-dependent manner ($P < 0.05$) (Fig. 7A and B). It was, therefore, inferred that NF- κ B regulates the expression of these pro-inflammatory factors in immune-mediated liver injury. To explore the enhancement in nitration caused by iNOS overexpression during immune-mediated liver injury, we assessed the levels of 3-NT, a

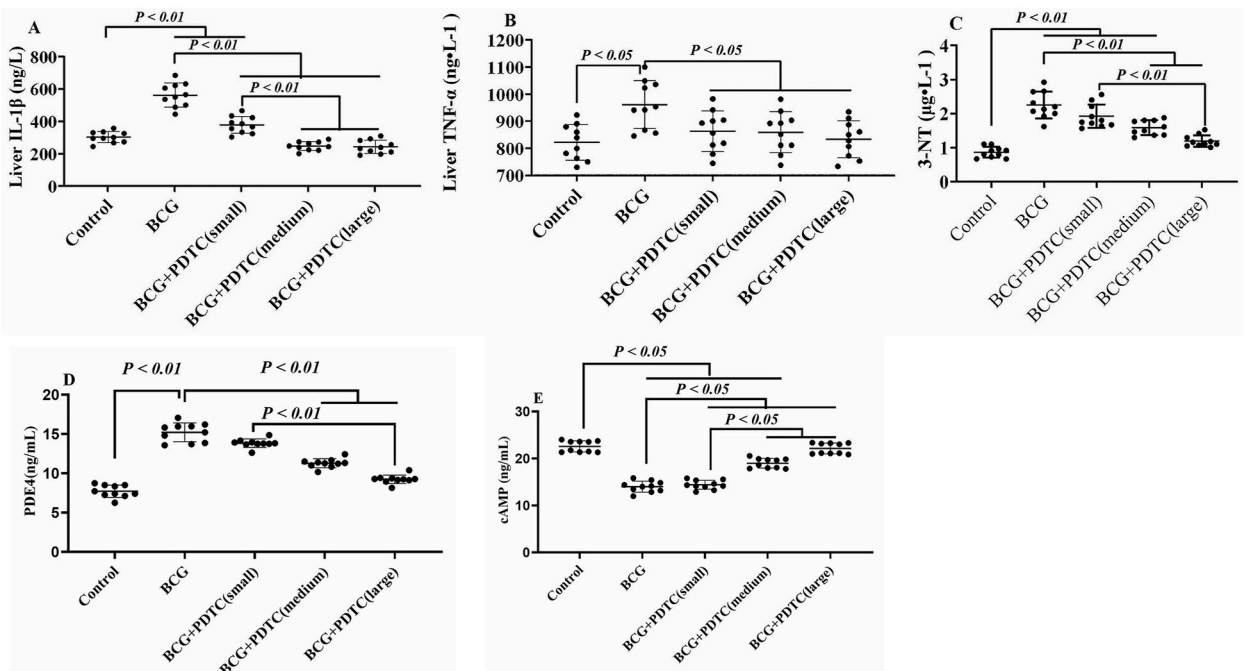


Fig. 7. Effects of ammonium pyrrolidine dithiocarbamate (PDTC) treatment on the expression of IL-1 β , TNF- α , 3-NT, phosphodiesterase (PDE4), and cAMP in rats with immune-mediated liver injury. Rats were administered injections of BCG (125 mg/kg, i.v. on day 1) or BCG (125 mg/kg, i.v. on day 1) + PDTC (25, 50, or 100 mg/kg/d, i.p. on days 11, 12, and 13). (A, B) PDTC treatment decreases the levels of TNF- α and IL-1 β in a dose-dependent manner ($P < 0.05$). (C) The BCG-treated group shows an elevated expression of 3-NT; however, PDTC treatment inhibits its high expression in a dose-dependent manner ($P < 0.05$). (D–E) In the BCG-treated group, the expression of PDE4 is significantly increased, whereas that of cAMP is significantly decreased in rat livers ($P < 0.05$). PDTC treatment reverses the process in a dose-dependent manner ($P < 0.05$). Data represent the mean \pm S.D. of $n = 10$ rats. P -values above scatter charts indicate differences between groups. Comparisons between groups were performed using one-way ANOVA followed by Tukey's test.

stable product that represents the strength of nitration. Similar to the above results, the BCG-treated group showed an elevated expression of 3-NT; however, PDTC treatment inhibited its high expression in a dose-dependent manner ($P < 0.05$) (Fig. 7C). The results indicated that the nitration process during immune liver injury is NF- κ B-dependent. The expression of PDE4 in rat livers in the BCG-treated group showed a significant increase, whereas the expression of cAMP was significantly decreased ($P < 0.05$). PDTC treatment reversed the process in a dose-dependent manner ($P < 0.05$) (Fig. 7D and E).

4. Discussion

We successfully replicated a rat model of acute hepatitis with immune liver injury characterised by the induction of inflammatory cells and the overexpression of inflammatory mediators. We could use PDTC to hinder NF- κ B activation leading to a transitory relief from inflammation. Proteomic results comprehensively describe the panorama of protein kinase, inflammatory cell pathway, NO pathway, and other protein changes during immune liver injury. The pharmacokinetic and molecular pharmacological experiments showed that CYP2E1 was downregulated via BCG-mediated immune stimulation, with selective inhibition of the recovery of NF- κ B activation. The downregulation of CYP2E1 involves iNOS-mediated nitration, and its recovery involves PKC-mediated CREB phosphorylation. The former is inflammatory activation, whereas the latter is inflammatory regression, and both are NF- κ B-dependent.

First, we found that the NF- κ B and CREB pathways regulate each other. Pharmacokinetic and molecular biology experiments confirmed that CREB and NF- κ B were overexpressed in BCG-induced liver injury. Inhibition of NF- κ B activation by PDTC can downregulate CREB, indicating that the two regulate each other in the inflammatory process. Inflammation and hypoxia activate CREB- and NF- κ B-mediated inflammation, coordinating immune response and tissue homeostasis [21–23]. CREB and NF- κ B may be the targets of phosphorylation mediated by PKC [24]. In addition, CREB activation is critical for the nuclear translocation of the p65 component of NF- κ B, which triggers a cascade of transcription factor activity [25]. CREB-binding proteins bind to NF- κ B [26], thus activating the NF- κ B pathway and inducing pro-inflammatory responses [27]. Our data support the idea that NF- κ B interacts with the CREB pathway and that activation of the NF- κ B pathway may inhibit the metabolic activity of CYP2E1, a prominent subtype of CYPs, by altering the expression patterns of CYP2E1 at both mRNA and protein levels.

Second, we also found that PKC regulates CREB phosphorylation via the NF- κ B pathway and is involved in the anti-inflammatory mechanism underlying immune-mediated liver injury. Both PKC and P-CREB are downregulated in BCG-induced liver injury, and inhibition of the overactivation of NF- κ B caused by PDTC can partially restore PKC activity, suggesting that PKC regulates CREB phosphorylation via the NF- κ B pathway. Notably, PKC is a central regulator of inflammatory signals and is involved in various signal transduction pathways. The regulation of its activity is implicated in inflammation, sepsis, and cancer, among other immunopathological conditions [28–30]. Previous studies have shown that PKC regulates NF- κ B activity in microglia. In addition, it is suggested to be involved in the induction of IL-1 β and TNF- α in microglia via the NF- κ B signalling pathway in response to lipopolysaccharide treatment [31,32]. Our results are similar to those of the above studies, except that the activation of PKC and P-CREB occurred during the inflammatory remission period. Notably, PKC may promote the phosphorylation of CREB-binding sites in the promoter region of CYP2E1 and inhibit CREB-binding, leading to substantial regulation of CYP2E1 activity in the liver. The metabolic activity and protein expression of CYP2E1 recovered to close to the normal level with the recovery of inflammation. It is reported that LPS induces NF- κ B translocation into the nucleus and its transcriptional activity, activation of cAMP/PKA signaling inhibits nuclear translocation of NF- κ B and negatively modulates NF- κ B transcriptional activity [33]. Our data support these ideas, and we further observe that inhibition of NF- κ B also reduce BCG-induced cAMP/PKC downregulation.

Third, we also found that iNOS-mediated nitration may be a critical cause of CYP2E1 downregulation during immune-mediated liver injury. Our results showed that iNOS was expressed mainly in the infiltrated mass of inflammatory cells and rarely in hepatocytes, indicating that iNOS was derived from these cells. PDTC improves inflammation by preventing NF- κ B translocation and reducing iNOS expression. iNOS is involved mainly in regulating the inflammatory process, with its expression regulated by NF- κ B, indicating that iNOS may regulate CYP2E1 through NF- κ B. Moreover, PKC binds to and activates NF- κ B, which induces the production of various inflammatory cytokines, such as TNF- α and IL-1 β . Inflammatory cytokines induce iNOS and catalyse guanidine on L-arginine to produce NO. They also react with O $_2^-$ and NO in liver tissue to form the potent oxidant peroxynitrite, thus enhancing post-translational nitration and further downregulating CYP2E1 [1,2,20,34]. In addition, NO relaxes blood vessels and improves hypoxia in inflamed liver tissue. In this study, we observed that BCG-mediated immune stimulation induced considerable amounts of iNOS and 3-NT in the liver. PDTC intervention reduces the production of iNOS and 3-NT and blocks the downregulation of CYP2E1. In addition, 3-NT is a stable biomarker for protein nitration. Together, these observations strengthen our hypothesis.

In addition to regulating CYP2E1 via the PKC/NF- κ B/CREB pathway, BCG-mediated immune stimulation also reduces oxidative stress, mitigates the damage caused by oxidative metabolites to liver cells, and performs self-regulation of homeostasis. Although our research confirms that the downregulation of CYP2E1 is governed primarily at the post-translational level during immune-mediated liver injury involving PKC-mediated CREB-phosphorylation and iNOS-mediated nitration, the regulation is multi-factorial involving other post-transcriptional regulatory mechanisms [2]. Our research has certain limitations that need to be addressed in future studies. In future experiments, we plan to conduct a detailed investigation to identify other mechanisms underlying CYP2E1 regulation.

In summary, during the process of immune-associated liver injury, the downregulation of protein and gene expression, metabolic activity of CYP2E1, and sharp rise in inflammatory cytokine levels in the liver are linked to PTMs, such as phosphorylation and nitration. PKC/CREB interacts with NF- κ B to co-regulate downstream inflammatory cytokines and the drug-metabolising enzyme CYP2E1. The regulation of drug metabolism is linked strongly to PKC/CREB-induced phosphorylation and iNOS-mediated nitration, both of which are NF- κ B-dependent.

5. Conclusions

We highlighted the post-transcriptional and post-translational regulation of CYP2E1 in immune-associated liver damage. In addition, CYP2E1 regulation could be an autonomous process that helps liver cells adapt to environmental changes, reduce oxygen consumption, alleviate further hypoxia in inflamed tissues, and minimise exposure to toxic and harmful metabolites. This regulation involves the action of CREB and its molecular target NF- κ B. The regulatory mechanism underlying the involvement of NF- κ B activity at the phosphorylation and nitration sites of CYP2E1 needs further evaluation.

Consent for publication

Not applicable.

Availability of data and materials

The datasets used or analysed during the current study are available from the corresponding author upon reasonable request, and they have been uploaded in the supplementary datasets file.

Ethics approval and consent to participate

All animal experiments complied with the ARRIVE Guidelines. The Ethics Committee of Baotou Medical College approved the study protocol (approval number: 2021-061). All experiments were conducted following the relevant guidelines and regulations. Sprague-Dawley rats were used as animal models in this study. All animals were assessed as healthy before starting the investigations. The animals were monitored before and after each injection to ensure no abnormalities in weight (>10%), appearance (fur), or behaviour (vocalisation, breathing, and movement). Every effort was made to limit animal suffering. Animals were handled by experienced researchers who ensured to minimise pre-execution stress.

Funding

This work was supported partly by the National Natural Science Foundation of China (No. 81460567, 82160709) and partly by the Inner Mongolia Natural Science Foundation of China (No. 2009MS1104, 2014MS0813, 2019MS08198) and the Project of the Department of Education of Inner Mongolia of China (No. NJ03148, NJZY13244).

CRedit authorship contribution statement

Huiqiong Zou: Investigation, Methodology, Writing – original draft. **Yingying Cao:** Supervision, Visualization. **Peipei Hao:** Investigation, Software, Validation. **Ziqi Jin:** Investigation, Resources. **Ruifeng Ding:** Data curation, Supervision. **Xuefeng Bai:** Methodology, Supervision. **Kun Zhang:** Data curation, Formal analysis, Supervision. **Yongzhi Xue:** Conceptualization, Formal analysis, Funding acquisition, Writing – review & editing.

Declaration of competing interest

The authors declare that they have no known competing financial interests or personal relationships that could have appeared to influence the work reported in this paper.

Acknowledgements

Not applicable.

Appendix A. Supplementary data

Supplementary data to this article can be found online at <https://doi.org/10.1016/j.heliyon.2023.e22641>.

References

- [1] E.T. Morgan, Impact of infectious and inflammatory disease on cytochrome P450-mediated drug metabolism and pharmacokinetics, *Clin. Pharmacol. Ther.* 85 (4) (2009) 434–438.
- [2] E.T. Morgan, et al., Physiological regulation of drug metabolism and transport: pregnancy, microbiome, inflammation, infection, and fasting, *Drug Metab. Dispos.* 46 (5) (2018) 503–513.
- [3] M. Aguiar, R. Masse, B.F. Gibbs, Regulation of cytochrome P450 by posttranslational modification, *Drug Metab. Rev.* 37 (2) (2005) 379–404.

- [4] Y.H. Li, H.C. Bi, M. Huang, [Effects of posttranslational modification on the activity of cytochrome P450: current progress], *Yao Xue Xue Bao* 46 (5) (2011) 487–492.
- [5] Q. Lin, et al., NF- κ B-mediated regulation of rat CYP2E1 by two independent signaling pathways, *PLoS One* 14 (12) (2019), e0225531.
- [6] Z.X. He, et al., Impact of physiological, pathological and environmental factors on the expression and activity of human cytochrome P450 2D6 and implications in precision medicine, *Drug Metab. Rev.* 47 (4) (2015) 470–519.
- [7] P. Beltrao, et al., Systematic functional prioritization of protein posttranslational modifications, *Cell* 150 (2) (2012) 413–425.
- [8] M. Ayati, et al., CoPhosK: a method for comprehensive kinase substrate annotation using co-phosphorylation analysis, *PLoS Comput. Biol.* 15 (2) (2019), e1006678.
- [9] M.A. Correia, et al., Hepatic cytochrome P450 ubiquitination: conformational phosphodegrons for E2/E3 recognition? *IUBMB Life* 66 (2) (2014) 78–88.
- [10] H. Ahsan, 3-Nitrotyrosine: a biomarker of nitrogen free radical species modified proteins in systemic autoimmunogenic conditions, *Hum. Immunol.* 74 (10) (2013) 1392–1399.
- [11] E. Billerbeck, et al., Mouse models of acute and chronic hepatitis B infection, *Science* 357 (6347) (2017) 204–208.
- [12] A. Filliol, et al., RIPK1 protects from TNF- α -mediated liver damage during hepatitis, *Cell Death Dis.* 7 (11) (2016), e2462.
- [13] Q. Fu, et al., Hepatic NK cell-mediated hypersensitivity to ConA-induced liver injury in mouse liver expressing hepatitis C virus polyprotein, *Oncotarget* 8 (32) (2017) 52178–52192.
- [14] N. van Montfort, et al., Hepatitis B virus surface antigen activates myeloid dendritic cells via a soluble CD14-dependent mechanism, *J. Virol.* 90 (14) (2016) 6187–6199.
- [15] T. Oinonen, K.O. Lindros, Zonation of hepatic cytochrome P-450 expression and regulation, *Biochem. J.* 329 (Pt 1) (1998) 17–35 (Pt 1).
- [16] F. Liu, et al., Involvement of NF- κ B in the reversal of CYP3A down-regulation induced by sea buckthorn in BCG-induced rats, *PLoS One* 15 (9) (2020), e0238810.
- [17] D. Li, et al., Glioma-associated human endothelial cell-derived extracellular vesicles specifically promote the tumorigenicity of glioma stem cells via CD9, *Oncogene* 38 (43) (2019) 6898–6912.
- [18] J. Massart, et al., Role of mitochondrial cytochrome P450 2E1 in healthy and diseased liver, *Cells* 11 (2) (2022).
- [19] X. Wang, et al., Effects of Ganoderma lucidum polysaccharide on CYP2E1, CYP1A2 and CYP3A activities in BCG-immune hepatic injury in rats, *Biol. Pharm. Bull.* 30 (9) (2007) 1702–1706.
- [20] J.D. Qin, et al., Effect of ammonium pyrrolidine dithiocarbamate (PDTC) on NF- κ B activation and CYP2E1 content of rats with immunological liver injury, *Pharm. Biol.* 52 (11) (2014) 1460–1466.
- [21] C. Baeck, F. Tacke, Balance of inflammatory pathways and interplay of immune cells in the liver during homeostasis and injury, *Excli j* 13 (2014) 67–81.
- [22] J. Nanduri, R.P. Nanduri, Cellular mechanisms associated with intermittent hypoxia, *Essays Biochem.* 43 (2007) 91–104.
- [23] H.K. Eltzschig, P. Carmeliet, Hypoxia and inflammation, *N. Engl. J. Med.* 364 (7) (2011) 656–665.
- [24] P. Regenhard, R. Goethe, L. Phi-van, Involvement of PKA, PKC, and Ca²⁺ in LPS-activated expression of the chicken lysozyme gene, *J. Leukoc. Biol.* 69 (4) (2001) 651–658.
- [25] M.T. Diaz-Meco, J. Moscat, The atypical PKCs in inflammation: NF- κ B and beyond, *Immunol. Rev.* 246 (1) (2012) 154–167.
- [26] J. Wang, et al., Histamine H3R antagonist counteracts the impaired hippocampal neurogenesis in Lipopolysaccharide-induced neuroinflammation, *Int. Immunopharm.* 110 (2022), 109045.
- [27] L. Cao, et al., Xuebijing protects against septic acute liver injury based on regulation of GSK-3 β pathway, *Front. Pharmacol.* 12 (2021), 627716.
- [28] S.Y. Fu, et al., PKC mediates LPS-induced IL-1 β expression and participates in the pro-inflammatory effect of A(2A)R under high glutamate concentrations in mouse microglia, *Neurochem. Res.* 44 (12) (2019) 2755–2764.
- [29] J. Yang, et al., Perfluorooctane sulfonate mediates microglial activation and secretion of TNF- α through Ca²⁺-dependent PKC-NF- κ B signaling, *Int. Immunopharm.* 28 (1) (2015) 52–60.
- [30] K.K. Haack, A.K. Mitra, I.H. Zucker, NF- κ B and CREB are required for angiotensin II type 1 receptor upregulation in neurons, *PLoS One* 8 (11) (2013), e78695.
- [31] B. Oesch-Bartlmowicz, F. Oesch, Modulation of mutagenicity by phosphorylation of mutagen-metabolizing enzymes, *Arch. Biochem. Biophys.* 423 (1) (2004) 31–36.
- [32] A.R. Aroor, D.E. Jackson, S.D. Shukla, Dysregulated phosphorylation and nuclear translocation of cyclic AMP response element binding protein (CREB) in rat liver after chronic ethanol binge, *Eur. J. Pharmacol.* 679 (1–3) (2012) 101–108.
- [33] T. Park, et al., N-Docosahexaenylethanolamine ameliorates LPS-induced neuroinflammation via cAMP/PKA-dependent signaling, *J. Neuroinflammation* 13 (1) (2016) 284.
- [34] Y. Du, et al., NF- κ B and enhancer-binding CREB protein scaffolded by CREB-binding protein (CBP)/p300 proteins regulate CD59 protein expression to protect cells from complement attack, *J. Biol. Chem.* 289 (5) (2014) 2711–2724.